

Determining Burgers vectors and geometrically necessary dislocation densities from atomistic data

Jun Hua and Alexander Hartmaier¹

Interdisciplinary Centre for Advanced Materials Simulation (ICAMS), Ruhr University Bochum, Stiepel Str. 129, 44801 Bochum, Germany

E-mail: Alexander.Hartmaier@rub.de

Received 23 November 2009, in final form 22 February 2010

Published 30 March 2010

Online at stacks.iop.org/MSMSE/18/045007

Abstract

We describe a novel analysis method to quantify the Burgers vectors of dislocations in atomistic ensembles and to calculate densities of geometrically necessary and statistically stored dislocations. This is accomplished by combining geometrical methods to determine dislocation cores and the slip vector analysis, which yields the relative slip of the atoms in dislocation cores and indicates the Burgers vectors of the dislocations. To demonstrate its prospects, the method is applied to investigate the density of geometrically necessary dislocations under a spherical nanoindentation. It is seen that this local information about dislocation densities provides useful information to bridge the gap between atomistic methods and continuum descriptions of plasticity, in particular for non-local plasticity.

1. Introduction

Nanoindentation is a widely used technique for probing mechanical properties locally in small volumes, as for example in precipitates [1] or thin films [2]. Classical continuum mechanics modeling is unable to comprehensively explain the mechanical response of a material during nanoindentation. In particular pop-in events or indentation size effects can only be understood on the atomic or microstructural scale. Molecular dynamics (MD) simulations, in contrast, have been shown to be a powerful tool for revealing the processes underlying the nanoindentation response and for providing valuable insights into material behavior [3]. The important goals of atomistic studies of nanoindentation are to identify the atomistic mechanisms of plastic

¹ Author to whom any correspondence should be addressed.

deformation under the indenter and to interpret indentation behavior on a microstructural scale, i.e. on the basis of dislocation nucleation and motion.

However, the complex datasets generated during the large-scale MD simulations, involving positions and potential energies of millions of atoms, make quantitative data analysis quite a challenge [4]. Several methods have been developed to identify crystal defects, in particular dislocations, by analyzing the geometrical configuration of local neighborhoods of atoms, e.g. the centrosymmetry method [5] and the common neighbor analysis [6]. The most recent and most powerful as well as robust method has been published by Ackland and Jones [7], who take advantage of the specific signature of different lattice types and crystal defects in the bond angle distribution (BAD) of each atom to analyze the local lattice configuration.

Furthermore, there exist several methods that are capable of evaluating local plastic slip from atomistic data: The slip vector analysis (SVA), developed by Zimmerman *et al* [8], compares the current atomic configuration with a reference state and thus quantifies the local atomic slip in the ensemble. The Burgers circuit method introduced to MD simulations by Stukowski *et al* [9] is capable of detecting dislocation cores and identifying Burgers vectors with only a local reference lattice, as opposed to the global reference lattice needed for the SVA. Finally, the Nye tensor analysis, as described by Hartley and Mishin [10], only needs the local lattice orientation to evaluate the Burgers vector, however, with a comparatively high numerical effort.

In the following section we describe a new method that enables Burgers vectors of dislocations to be calculated immediately from atomistic data sets resulting from MD simulations. The method is applied to the simple test case of a single dislocation in a face centered cubic (fcc) crystal as well as to a complex dislocation configuration underneath a nanoindentation. Then the method of Burgers vector analysis is applied to calculate signed dislocation densities, i.e. densities of geometrically necessary dislocations (GNDs), during nanoindentation in an fcc metal. Before the results are summarized, we demonstrate in terms of an outlook that the method needs to be further refined in order to perform a Burgers vector analysis in non-close-packed body centered cubic (bcc) crystals.

2. Burgers vector analysis

2.1. Method

As mentioned above, in this work the SVA is used as a measure of local plastic deformation and its relation to the Burgers vectors of the lattice dislocations that caused this plastic slip is exploited. The SVA method has been shown to be capable of detecting different contributions to plastic slip from atomistic simulations [11, 12]. The slip vector \mathbf{s} of atom k is defined as

$$\mathbf{s}^{(k)} = -\frac{1}{n_s} \sum_{l=1}^n (\mathbf{x}^{(kl)} - \mathbf{X}^{(kl)}), \quad (1)$$

where n is the number of nearest neighbors of atom k , n_s is the number of the slipped neighbors, $\mathbf{x}^{(kl)}$ and $\mathbf{X}^{(kl)}$ are the position difference vectors between atom k and l in the current and in the reference configuration, respectively. The reference configuration denotes the arrangement of atomic positions at the beginning of the deformation step.

The slip vector is a measure of the local plastic deformation since it denotes the average displacement of an atom in its current position compared with the initial position and relative to its nearest neighbors. However, the slip vectors of atoms that lie on opposite sides of the

slip plane point in opposite directions (cf figure 1(b)). Hence, we have to develop a way to uniquely define the direction of the slip vector, before we can associate it with plastic slip in the crystal. To accomplish this, we identify the atoms situated in dislocation cores with the help of the BAD method and only analyze the slip vector within the dislocation core. Furthermore, by identifying those atoms with a higher coordination number than bulk atoms, we can identify the atoms in the core of an edge dislocation that lie on the side of the slip plane where it intersects the inserted half plane of atoms that is terminated by the dislocation line. In fcc crystals, we typically find atoms with coordination numbers of 13 on this side of the slip plane. On the opposite side of the slip plane, in contrast, we find atoms with coordination numbers of 11, i.e. with smaller coordination numbers than bulk atoms. By using this property of edge dislocations that allows us to define an ‘upper’ and ‘lower’ side of the slip plane, we are able to define a unique direction of the plastic slip that is characterized by the slip vector of atoms in the dislocation core.

2.2. Analysis of a single dislocation

To demonstrate the method, a copper crystal with 97 296 atoms containing a single edge dislocation is studied here. For simplicity, and since we only want to demonstrate the analysis method, we use rather simple geometry of a box with side lengths of 202.8 Å times 53.0 Å times 106.4 Å. The top surface is a crystallographic (1 1 1) plane with free boundary conditions, the bottom surface is fixed and periodic boundary conditions are applied to the sides of the simulation box. The simulations using an embedded atom method (EAM) potential for Cu developed by Mishin *et al* [13] are conducted in the NVE ensemble (constant number of atoms, constant volume, constant energy). The MD simulations were performed using a version of the IMD parallel MD code [14] in which we implemented the BAD and SVA methods. For visualization, the atomistic configuration viewer Atomeye [15] was used. Before mechanically loading the simulation box, the dislocation has been properly relaxed, until all atoms found their energetic minimum positions, which corresponds to a temperature of $T = 0$ K. Finally the relaxed ensemble is loaded with a shear stress of 300 MPa in a dynamic simulation. During this simulation, the edge dislocation glides on the (1 1 1) plane under the action of the applied shear stress.

In figure 1(a) the atomic configuration and the results of the BAD analysis are shown for the atoms in the vicinity of the dislocation above and below the slip plane. As it is well known, an edge dislocation in the fcc crystal structure is dissociated into a leading and a trailing Shockley partial linked by a stacking fault. The dissociation reaction for copper is given by $a/2[\bar{1} 1 0] = a/6[\bar{1} 2 \bar{1}] + a/6[\bar{2} 1 1]$. The lattice constant of copper is $a = 3.615$ Å, which yields a Burgers vector magnitude for copper of $b_{\text{partial}} = 1.48$ Å for a $\{1 1 1\}\langle 1 1 2 \rangle$ partial dislocation and $b_0 = 2.56$ Å for a perfect $\{1 1 1\}\langle 1 1 0 \rangle$ dislocation.

In figure 1(b) the result of the SVA for the atoms lying below and above the slip plane is shown. In figure 1(c) we combine the BAD and the SVA method, which allows us to filter out the slip vector of only the atoms lying in the dislocation core. Furthermore, in figure 1(c) the sign of the slip vectors lying above the slip plane has been flipped, such that all vectors point in the same direction. These vectors thus give an atomistic representation of the Burgers vector of the dislocation.

In figure 1(b), there are four groups of atoms represented by the slip vectors: (i) atoms lying in the wake of the dislocation with a full Burgers vector as slip vector (red), (ii) atoms in the stacking fault region with a partial Burgers vector as slip vector (orange), (iii) atoms in the leading partial dislocation core and (iv) atoms in the trailing partial dislocation core (green, pink and blue). Since within each group the slip vectors are almost identical, here only one

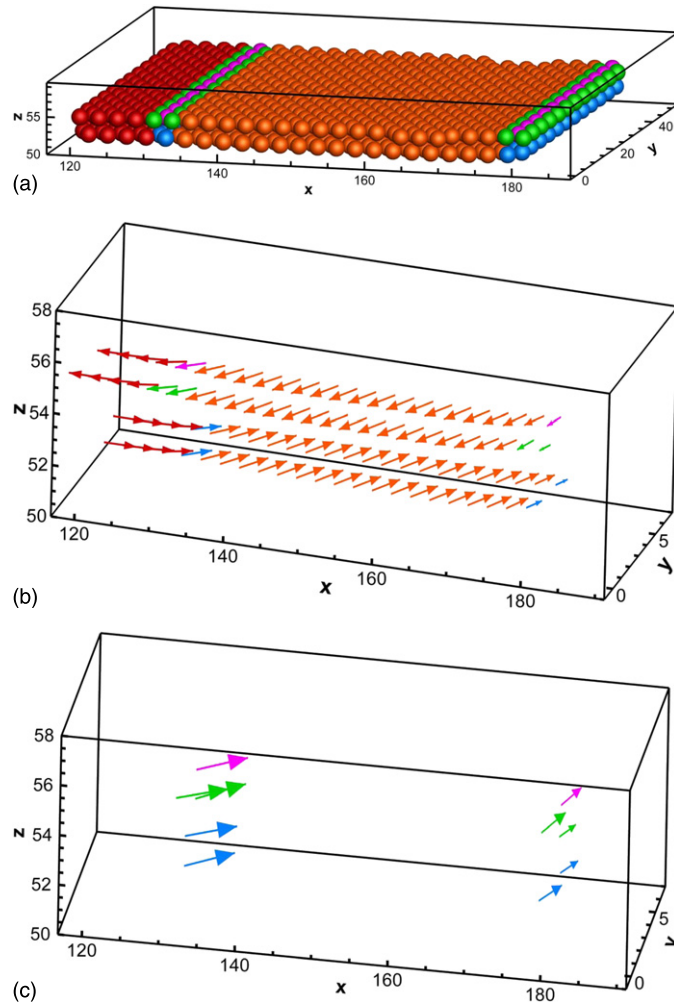


Figure 1. Atomistic configuration of an edge dislocation and its Burgers vector analysis. (Units in Å; color code: red: fcc, orange: stacking fault, green: 12 neighbors, no symmetry, blue: 11 neighbors, pink: 13 neighbors). (a) Result of the BAD analysis of atoms close to the dislocation. (b) Results of SVA represented as arrows; (c) Atomistic Burgers vectors of the atoms lying in the dislocation core.

atom of a group is analyzed further. This closer analysis shows that the atoms in the stacking fault region have slip vectors of $(-1.19, 0.61, 0.58)$ in the coordinate system spanned by the crystallographic orientations $[100]$, $[010]$ and $[001]$. The magnitude of this slip vector is 1.46 \AA , which is very close to the magnitude of the partial Burgers vector b_{partial} . The direction of this slip vector is close to $(-1.0, 0.5, 0.5)$ that corresponds to the crystallographic direction of the $[\bar{2}11]$ Burgers vector of the leading Shockley partial. The slip vectors of the atoms in the dislocation core are not in such good agreement with the expected full Burgers vectors. This is seen by the analysis of an atom in the trailing partial core, which has the slip vector components $(-1.41, 1.19, 0.32)$. The direction of this slip vector is reasonably close to the $(-1.0, 1.0, 0)$ vector, i.e. the complete Burgers vector. However, the magnitude of this slip vector is 1.87 \AA and thus smaller than b_0 , which shows that the lattice slip is still incomplete

within the dislocation core. Although the slip vectors of the atoms in the dislocation cores are thus not identical to the true crystallographic vectors, they approximate the true vectors sufficiently, such that a reconstruction of the true Burgers vector is possible without ambiguity.

2.3. Analysis of nanoindentations

Large-scale MD simulations of nanoindentation of a Cu single crystal are performed in an ensemble consisting of 2 448 000 atoms with the size of $301 \times 306 \times 317 \text{ \AA}^3$. The (1 1 1) top surface of the crystal is indented by a rigid spherical indenter with the radius of 80 \AA . The MD simulations have been carried out at $T = 30 \text{ K}$ in a thermostated ensemble. Details of the indentation method can be found in [3], here we only focus on the analysis of the plastic zone that develops during the indentation process.

Figure 2 shows a snapshot of the dislocation configuration at an indentation depth of $h = 21 \text{ \AA}$, representing the different analysis methods. In figure 2(a) the dislocation structure is determined by the BAD analysis and it can be seen how the dislocations are spread into Shockley partials, as expected for an fcc crystal. Figure 2(b) shows the combination of BAD and SVA for the same snapshot. It is seen that the arrows indicating the slip vector point in opposite directions above and below the slip plane. Nonetheless, even in this representation edge and screw dislocation segments can be discriminated by the slip vectors pointing orthogonal or parallel to the line direction of the dislocation, respectively. In figure 2(c) only atoms are displayed that have a slip vector corresponding approximately to a full Burgers vector in the sense of the discussion at the end of the previous section. This gives a simplified representation of the dislocation configuration. Finally, figures 2(d) and (e) reveal blow-ups of details in figure 2(b), marked with A and B, respectively. Note that here a full Burgers vector analysis has been employed, i.e. the slip vectors below the slip plane have been flipped to indicate in a unique direction. Even in this complex situation almost all of the slip vectors can be made to point in a unique direction by the method described above. In figure 2(d) the atom indicated with ‘C’ is located on an edge segment and has the slip vector of $(-1.38, -1.11, 0.33)$ with the magnitude of 1.80. The direction of this slip vector is identified as the crystallographic $[\bar{1} \bar{1} 0]$ direction, i.e. a full Burgers vector, which means that the dislocation is a trailing partial. In another segment shown in figure 2(e) atom ‘D’ has the slip vector of $(0.30, 0.60, 0.37)$, corresponding to the crystallographic $[1 2 1]$ direction. This indicates that this dislocation segment belongs to a leading Shockley partial. Since the slip vector is parallel to the dislocation line, this dislocation segment is of screw type. It is interesting to note here that our projection method to select a unique direction of the slip vector works due to the small edge components of the Shockley partials even in nominally perfect screw dislocations.

3. Calculation of vectorial dislocation densities

In the above section we demonstrated that the developed Burgers vector analysis method is capable of characterizing dislocation structures in complex atomistic ensembles. In this section it is shown that with this information gathered from the atomistic structure a vectorial dislocation density can be calculated that corresponds to the density of GNDs. The total (scalar) dislocation density is defined as the total length of all dislocation segments per volume. For the atomistic data the length of the dislocation segments is not *a priori* known, but from figure 2 it becomes evident that each detected atom in the dislocation core can be attributed an effective segment length $l_0 = 1.0 \text{ \AA}$ that it represents. This length corresponds to the average distance of atoms along the dislocation line and is smaller than the nearest neighbor distance, because the dislocation line consists of two parallel rows of atoms. Hence we define the total dislocation

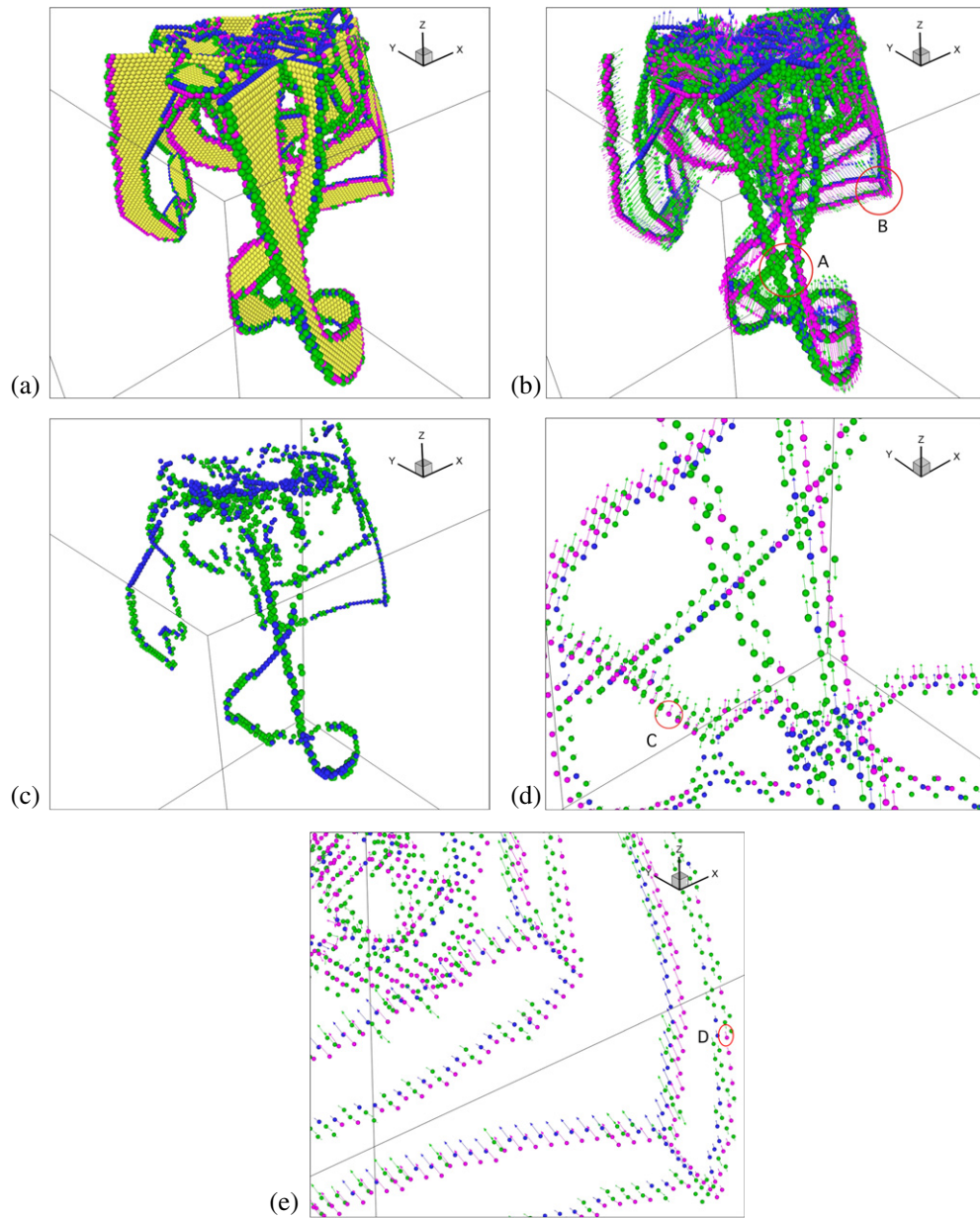


Figure 2. Dislocation structure under a nanoindentation. (same color code as figure 1) (a) Dislocation structure characterized with BAD method. (b) Combination of BAD and SVA, where slip vectors are represented by arrows. (c) Full dislocation lines. (d) Edge dislocation (zoom in of region A in (b)). (e) Screw dislocation (zoom in of region B in (b)).

density as

$$\rho_T = \frac{l_0 N_{\text{atom}}}{V}, \quad (2)$$

where N_{atom} is the number of identified dislocation core atoms per volume V . While the total dislocation density counts all dislocations in a given volume, the GND density does not consider

dislocations of opposite Burgers vectors, i.e. dislocation dipoles or loops, because they do not produce strain gradients or lattice rotations [16]. Thus we define the GND density as

$$\rho_G = \frac{l_0}{V} \left\| \sum_{i=1}^{N_{\text{atom}}} \frac{\mathbf{s}_i}{\|\mathbf{s}_i\|} \right\| \quad (3)$$

which means that for each atom in the dislocation core we add a unit vector in the direction of the Burgers vector. Hence we achieve that dislocation dipoles or loops within the control volume cancel out and do not contribute to this dislocation density, as desired. By the use of unit vectors it is achieved that the measured GND density is insensitive to statistical variations in the lengths of the slip vectors. We note that in principle it would be possible to define the GND density for leading or trailing partials independently. However, the definition given here yields the best statistics and hence the smallest scatter of the results. For completeness we define the density of statistically stored dislocations (SSDs) as $\rho_S = \rho_T - \rho_G$.

Note that by definition the GND density is scale dependent, because dislocations are nucleated as loops that expand thereafter. Thus, if the control volume extends over the entire crystal, only the dislocation segments opposite to those who left the crystal at free surfaces will contribute to the GND density, whereas for smaller control volumes all segments opposite to segments that left this control volume will contribute to the GND density. This means that the control volumes have to be chosen with care.

Further sources of errors in the GND densities are stemming from the ambiguity of the slip vectors of atoms that lie on previously slipped planes. Since we only consider momentary snapshots, however, this distortion only affects a few individual atoms along the dislocation line, such that this error is very small. Furthermore, the projection method to yield a unique direction of the slip vector also fails for a few individual atoms. The largest source of error, however, is the effective segment length l_0 of an atom. This quantity can only be estimated and may also vary locally along a dislocation segment. We, furthermore, observed that above approximately 300 K the thermal fluctuations of the atoms cause erroneous detections of defect atoms by the BAD method, which interferes also with the Burgers vector analysis.

Nix and Gao [17] attributed the indentation size effect to the strain gradient under the indenter caused by plastic deformation of the indented surface. The GNDs that are needed to create this strain gradient cause an additional hardening that depends on the indentation depth. Because the volume of the plastic zone under small indents is smaller and hence the GND density is higher, the material appears to be harder for smaller indents. In their work, Nix and Gao assumed the plastic zone for a conical indenter to be a hemispherical region below the projected contact area with the same extension as the contact radius a_c of the indenter. In subsequent work of Durst *et al* [18] it was shown that this assumption is somewhat inconsistent and that a good agreement of model and experiment is achieved when a larger plastic zone size $a_{\text{pz}} = 1.9a_c$ is assumed. Generally, the radius of the plastic zone is approximated by $a_{\text{pz}} = f a_c$, where f is a dimensionless material dependent constant ranging approximately from 0 to 3.5.

With the analysis method presented above it is possible to calculate the spatial variation of the GND density under a nanoindentation from large-scale MD simulations, i.e. without any *a priori* assumptions on plasticity. To accomplish this we evaluate the GND density in concentric volumes V around the indentation point. Hence, as shown in figure 3, the control volume enclosed in a radius R in which the dislocation densities are evaluated is given by

$$V(R) = 2\pi R^3/3 - V_{\text{ind}}, \quad (4)$$

where $V_{\text{ind}} = \pi h^2(r - h/3)$ is the volume displaced by the indenter of radius r at indentation depth h .

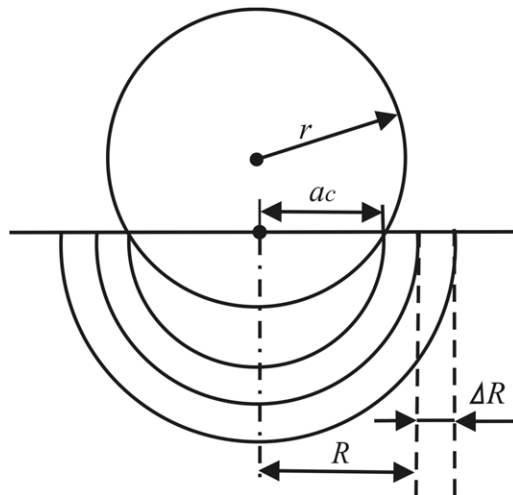


Figure 3. Sketch of the geometry of the evaluation volumes for the dislocation densities in the form of concentric shells.

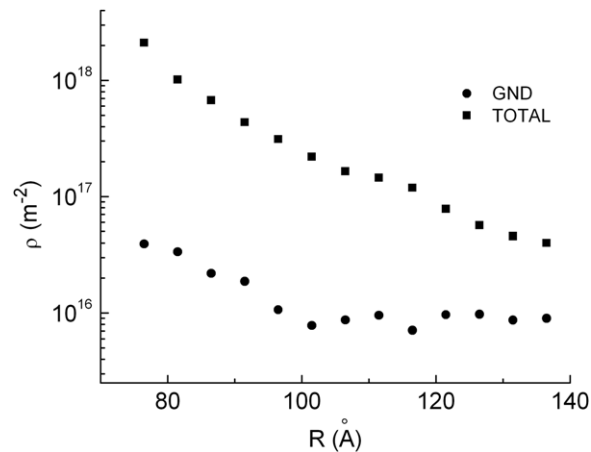


Figure 4. Local variation of dislocation densities. Total dislocation density and GND density in concentric shells plotted against distance from the indentation point.

Figure 4 shows the dislocation densities evaluated in concentric shells of thickness $\Delta R = 5 \text{ \AA}$ with volumes $V(R + \Delta R) - V(R)$ at an indentation depth of $h = 35 \text{ \AA}$ of a spherical indenter with radius $r = 80 \text{ \AA}$. It is seen that the total dislocation density decreases constantly with increasing R , while the GND density starts off at a rather high level and sinks to an almost constant value within a distance of $R = 104 \text{ \AA}$. This distance consequently defines the size of the plastic zone around the indenter. For comparison, the contact radius of the indentation is $a_c = 65 \text{ \AA}$ at this indentation depth, i.e. the size of the plastic zone is roughly 1.6 times larger than the contact radius, in good agreement with the results of Durst *et al* [18]. It is noted here that the constant GND density even for large distances from the indenter must be attributed to the finite size of the simulation box and the boundary conditions that cause dislocations to pile up against the lower edge of the simulation box.

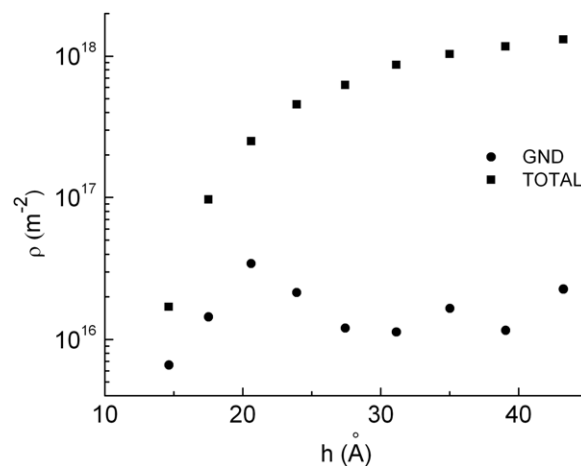


Figure 5. Variation of dislocation density with indentation depth. Total dislocation density and GND density within the plastic zone as a function of indentation depth.

The dislocation densities within the hemisphere defined by the contact radius of the indenter are studied at different indentation depths in figure 5. It is seen that the total dislocation density increases, while the GND density stays rather constant, as it is expected for a spherical indentation with a constant radius of curvature. The ratio between the size of the plastic zone and the contact radius slowly decreases from a value of 2 down to 1.5 during the spherical indentation.

4. Outlook: Burgers vector analysis of bcc materials

In this section the system modeled is a tungsten bi-crystal with a low angle grain boundary. We choose this model in order to investigate the experimentally observed grain boundary proximity effect [19] by simulating the load-displacement response near and away from a grain boundary. In this paper, we only use this model to test the Burgers vector analysis method for a bcc crystal. A more detailed analysis of this grain boundary problem will be published elsewhere.

The interatomic interactions are described by the Finnis–Sinclair potential for tungsten [20]. Nanoindentation is conducted as before with a spherical indenter onto a (001) surface of bcc tungsten. The dimensions of the simulation box are $405 \text{ \AA} \times 202.6 \text{ \AA} \times 300 \text{ \AA}$, with lateral periodic boundary conditions, a free top surface and fixed z -displacements of atoms close to the bottom surface. The radius of the spherical indenter used in our simulations is 80 \AA . The simulations were performed in the NVE ensemble, i.e. with a constant energy in the sample. The time step is 1 fs. These details are only provided for completeness, in this work the nanoindentation method only serves to generate a non-trivial atomistic configuration for the Burgers vector analysis.

Figure 6 shows the atomic configuration beneath the indenter at the indentation depth of 20 \AA and the corresponding slip vectors, respectively. It is seen that the small angle grain boundary is represented by a checkerboard network of screw dislocations. The mobile dislocations in the plastic zone of the nanoindentation can be identified with sufficient precision by the BAD method and it is seen that the dislocation cores are spread on the glide planes. In contrast to the fcc metal, no dislocation dissociation into partials is taking place. However, in the non-close packed bcc structure there is no clear signature of atoms sitting on the same

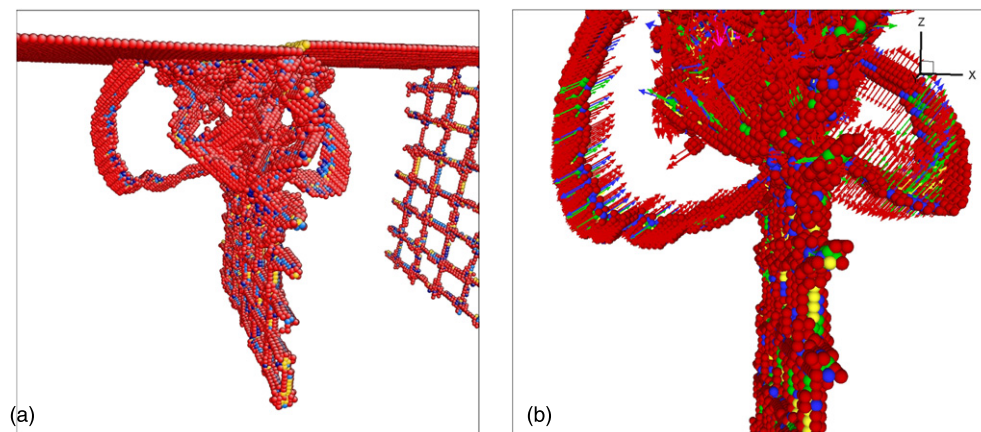


Figure 6. Atomistic configuration under a nanoindentation in a bcc tungsten bi-crystal (a) and corresponding SVA of atoms in the dislocation cores (b).

or opposite side of the inserted half plane, as in the case of the close-packed fcc materials. Since the slip vectors of atoms with identical BAD values or coordination numbers point in the opposite directions, a simple projection method of the slip vectors to yield the direction of the Burgers vector, as discussed above, does not seem possible in bcc structures and possibly also other non-close-packed materials.

5. Summary

Through the above analysis we have successfully identified Burgers vectors in close-packed fcc metals purely from atomistic data. The principle of the method is shown on a sample containing a single edge dislocation, while the full power of the method is demonstrated in the analysis of a large-scale atomistic simulation of nanoindentation into a Cu single crystal. This complex analysis is accomplished by combining the slip vector analysis [8] and the bond angle distribution method [7] with a newly developed method to project the direction of the slip vector into a unique direction, i.e. the direction of the Burgers vector. The knowledge about the local distribution of lattice defects and their Burgers vectors has been exploited to calculate the total dislocation density as well as the vectorial dislocation density representing the density of geometrically necessary dislocations. These quantities in turn represent the link between atomistic scale models and continuum descriptions of material behavior. While this method yields reliable results for Burgers vectors in close-packed metals, the projection is not possible in bcc crystals, where alternative methods need to be developed.

Acknowledgments

The authors gratefully acknowledge the financial support through ThyssenKrupp AG, Bayer MaterialScience AG, Salzgitter Mannesmann Forschung GmbH, Robert Bosch GmbH, Benteler Stahl/Rohr GmbH, Bayer Technology Services GmbH and the state of North-Rhine Westfalia/Germany as well as the European Commission in the framework of the European Regional Development Fund (ERDF).

References

- [1] Göken M and Kempf M 1999 *Acta Mater.* **47** 1043–52
- [2] Gouldstone A, Chollacoop N, Dao M, Li J, Minor A M and Shen Y L 2007 *Acta Mater.* **55** 4015–39
- [3] Ziegenhain G, Hartmaier A and Urbassek H M 2009 *J. Mech. Phys. Solids* **57** 1514–26
- [4] Buehler M J, Hartmaier A, Gao H, Duchaineau M and Abraham F F 2004 *Comput. Methods Appl. Mech. Eng.* **193** 5257–82
- [5] Kelchner C L, Plimpton S J and Hamilton J C 1998 *Phys. Rev. B* **58** 11085–8
- [6] Honeycutt J D and Andersen H C 1987 *J. Phys. Chem.* **91** 4950–63
- [7] Ackland G J and Jones A P 2006 *Phys. Rev. B* **73** 054104
- [8] Zimmerman J A, Kelchner C L, Klein P A, Hamilton J C and Foiles S M 2001 *Phys. Rev. Lett.* **87** 165507
- [9] Stukowski A and Albe K 2010 *Modelling Simul. Mater. Sci. Eng.* **18** 025016
- [10] Hartley C S and Mishin Y 2005 *Acta Mater.* **53** 1313–21
- [11] Vo N Q, Averback R S, Bellon P, Odunuga S and Caro A 2008 *Phys. Rev. B* **77** 134108
- [12] Brödling N C, Hartmaier A, Buehler M J and Gao H 2008 *J. Mech. Phys. Solids* **56** 1086–104
- [13] Mishin Y, Mehl M J, Papaconstantopoulos D A, Voter A F and Kress J D 2001 *Phys. Rev. B* **63** 224106
- [14] Stadler J, Mikulla R and Trebin H R 1997 *Int. J. Mod. Phys. C* **8** 1131–40
- [15] Li J 2003 *Modelling Simul. Mater. Sci. Eng.* **11** 173–7
- [16] Gao H, Huang Y, Nix W D and Hutchinson J W 1999 *J. Mech. Phys. Solids* **47** 1239–63
- [17] Nix W D and Gao H 1998 *J. Mech. Phys. Solids* **46** 411–25
- [18] Durst K, Backes B and Göken M 2005 *Scr. Mater.* **52** 1093–7
- [19] Lilleodden E T, Zimmerman J A, Foiles S M and Nix W D 2003 *J. Mech. Phys. Solids* **51** 901–20
- [20] Finnis M W and Sinclair J E 1984 *Phil. Mag.* **50** 45–55